Chemistry and Materials

The Centre for Science Innovation

Research Article

Chem. Mater. 1 (1) 2022, 1-6

Electrodeposition of PANI-NiO as Electrode for Deionization K^+ and Cl^-

Annisa Auliya[1], Raka Dwi Deswara[2], Maria Paristiowati[3], Setia Budi[2,*]

[1]The Centre for Science Innovation, Jl. Utan Kayu Raya, Jakarta 13120, Indonesia

[2]Department of Chemistry, Faculty of Mathematics and Natural Sciences, Universitas Negeri Jakarta, Jl. Rawamangun Muka, Jakarta 13220, Indonesia

[3]Department of Chemistry Education, Faculty of Mathematics and Natural Sciences, Universitas Negeri Jakarta, Jl. Rawamangun Muka, Jakarta 13220, Indonesia

*Corresponding author: setiabudi@unj.ac.id

RECEIVED
10 November 2021

ACCEPTED
30 January 2022

PUBLISHED ONLINE
28 February 2022

Abstract

This study aims to synthesize thin film of polyaniline-nickel oxide (PANI-NiO) as an electrode in capacitive deionization (CDI) technology. Thin film PANI-NiO were synthesized by electrodeposition method with different applied potentials. The FTIR spectrum and XRD pattern confirmed that PANI-NiO has been successfully synthesized. Based on the SEM-EDX data, PANI-NiO has a tightly stacked granular morphology, which consist of Fe, Cr, S, Ni, O, and C elements. Based on experimental results, the highest capacitance come from PANI-NiO 1.25 V with a value of 475.24 F/g. PANI-NiO 1.25 V also has a small resistance, which is 13.55 Ω. Salt reduction efficiency test for PANI-NiO 1.25 V also shows the highest salt reduction efficiency compared to other electrodes. Owing to its high capacitance, low charge transfer resistance, and high salt reduction capacity, the PANI-NiO prepared at 1.25 V might be a potential material to be developed for the electrolyte deionization application.

Keywords: PANI-NiO, electrodeposition, capacitive deionization, desalination, conductive polymers, capacitance

1. Introduction

More than 96.5% of the water on earth is in the oceans and seas, but due to the presence of salt which makes it salty, the water in the oceans is unsuitable for drinking. Only about 2.5% of all water on earth is fit for drinking, which means it can be used directly by humans, animals, and plants. In reality, only about 0.65% of water is available and suitable for living on earth. The remaining 1.95% of water is trapped in glaciers and snowfields [1]. As the population increases, the need for water also go up. This can lead to water pollution caused by human activities. The quantity of wastewater and pollution are steadily increasing worldwide. Alternatives such as desalination technology are the right choice to provide clean water reserves. Previously, some desalination methods have been developed, including distillation, reverse osmosis, electrodialysis, and capacitive deionization [2].

Capacitive deionization (CDI) is an electrochemically controlled method for removing salts from aqueous solutions by taking advantage from the excess ions adsorbed in the double layer region at the electrode solution interface when the electrodes are electrically charged by an external power supply [3]. CDI is efficient and environmentally benign when compared to traditional technologies such as distillation, electrodialysis, reverse osmosis, or other desalination technologies [2,4,5,6]. Factors that affect the adsorption ability of an electrode to improve CDI technology include surface area, pore distribution, pore size, and the conductivity of the electrode constituent materials. One alternative material that can be used as an electrode is a conductive polymer.

Polyaniline (PANI) is a conductive polymer that has been studied recently because it has unique physical and chemical properties, so it can be used for various applications. PANI has several advantages, such as easy to synthesize, high electro-activity properties, low density, high electrical conductivity, and good environmental stability [7,8]. To improve electrochemical properties in the form of capacitance and impedance, innovation is

needed in terms of combining PANI with other materials such as metals.

Metals such as Fe, Ni, Cu, and Ti combined with PANI can increase the electro-activity of the material and the performance of CDI [9,10]. In this research, Ni metal oxide doping will be carried out on PANI. Nickel oxide (NiO) has been widely studied because of its high specific capacitance, large surface area, and low cost. In particular, NiO is an electrode material capable of being used for supercapacitor applications along with many other applications such as fuel cells, catalysis, gas sensors, and electrochromic films [8].

Various methods have been carried out for the synthesis of PANO-NiO. Navale et al., 2018 synthesized PANI-NiO by electropolymerization method which was applied as a supercapacitor, resulting in a capacitance of 936.3 F/g. Other methods have also been widely reported in the PANI-NiO synthesis, but these methods have weaknesses such as the process that takes a long time and the use of materials that are less efficient. Electrodeposition is an alternative method to synthesize PANI and PANI-NiO which is faster and has good results [11,12]. In this research, PANI-NiO film synthesis will be carried out through electrodeposition by varying the potentials which is expected to affect morphology, capacitance, impedance, and deionization performance of the material.

2. Materials and Method

PANI-NiO were synthesized using an electrodeposition method that utilised a three-electrode cell. A platina wire, Ag/AgCl electrode, and stainless steel 304 were used as the counter, reference, and working electrode, respectively. Electrodeposition was controlled using eDAQ potensiostat (EA 163) by potensiostatic mode in electrolytes containing 0.5 M aniline in 0.5 M H_2SO_4 added with 0.5 M $NiSO_4.5H_2O$. This synthesize experiment was carried out at 1.00 V, 1.25 V, 1.50 V, 1.75 V, and 2.20 V for 3 minutes. After deposition, deposit was rinsed with distilled water and dried at room temperature.

Samples were characterized with a fourier transform infrared (FTIR) spectroscope and X-ray diffractometer (XRD) to identify its functional group and crystallinity, respectively. Micrographs and element composition of the samples were taken using a scanning electron microscope and energy dispersive X-ray spectroscope (SEM-EDX). Electrochemical behaviours were examined using electrochemical impedance spectroscopy and cyclic voltammetry in an electrolytes containing 0.5 M KCl. Finally, the capacity deionization test conducted by triangle technique between 0.3 and 0.9 V in 0.3 M KCl for 30 minutes. Then, the solution that used for latter experiment tested by conductometer every 15 seconds and its results used as a salt reduction parameter based on **Eq. 1**:

$$\% \text{ Salt Reduction} = \frac{\sigma f - \sigma p}{\sigma f} \times 100\% \quad \textbf{(Eq. 1)}$$

where the σ_f is final conductivity and σ_p represents initial conductivity.

3. Results and Discussion

3.1 FTIR Characterization

In Figure 1, FTIR spectra of the synthesized PANI and PANI-NiO have been shown. Figure 1a indicates absorption characteristics of PANI by the existence of the peaks of N-H, C-H, C=C (Q), C-H, and N=Q=N that are assigned as follows. A peak observed at the 3423 cm^{-1} was a typical strain bond from N-H [13]. Peaks at 2918 cm^{-1} and 1559 cm^{-1} represented C-H strain [12] and C=C quinoid strain in benzene [14], respectively. Peak at 1492 cm^{-1} were related to C-H deformation. Peak at 1197 cm^{-1} were associated to N=Q=N group [15]. And peak at 740 cm^{-1} were attributed to vibration bond from C-H. These spectra confirmed that PANI has been formed.

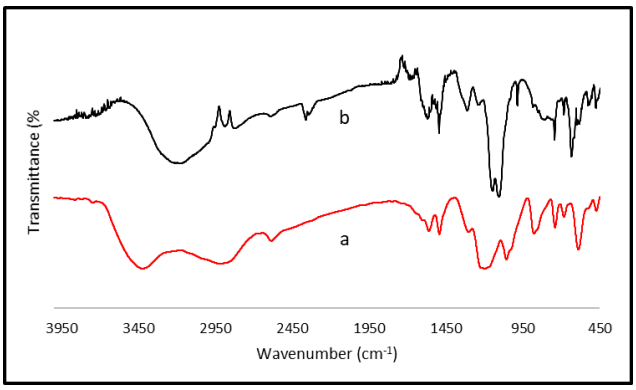

Figure 1. FTIR spectra of PANI-NiO

Figure 1b shows PANI-NiO spectra that confirmed by the existence of the characteristics peaks of N-H, C=C (Q), C-H, C-N, N=Q=N, and NiO that are assigned as follows. A peak observed at the 3197 cm^{-1} were related to N-H strain. Peak at 1577 cm^{-1} were due to typical band from C=C quinoid in benzene. Peak at 1492 cm^{-1} were due to C-H deformation [16]. Peak emerged at 1242 cm^{-1} was assigned to C-N vibration. Peaks at 1153 and 825 cm^{-1} were related to C-H aromatic bending for 1,4-disubstitution ring aromatic [13]. Peak at 1099 cm^{-1} was associated with N=Q=N (Q was representation from quinoid). Peak at 744

cm^{-1} was represented bending vibration from C-H [17]. Meanwhile, peaks that indicate NiO was emerged at 632 and 474 cm^{-1} [9]. From these spectra, we can see that some peaks were shifting, caused by coordination between organic and inorganic materials from N-H strain vibration [16].

3.2 XRD Characterization

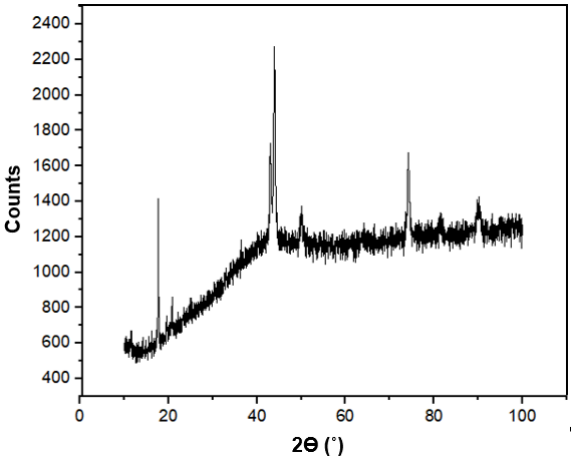

Figure 2. Diffraction pattern of PANI-NiO

Figure 2 shows the XRD pattern of PANI-NiO. Diffraction peaks at 2θ 17.67°, 20.74°, and 25.86° show the formation of the PANI emeraldine salt phase. These peak were the main peak from PANI diffraction [18,19,20]. Furthermore, peak represents NiO was emerged at 36.41°, 43.03°, and 62.83° which reflected (002), (111), and (002) crystals. In addition, peak at 43.98° represents Ni which formed because the appropriate potential condition that supported this metal formation. Based on this data, we can conclude that PANI-NiO has been successfully synthesized in this experiment.

3.3 SEM-EDX Characterization

Figure 3 shows that PANI-NiO has a dense granular morphology and there are object attached to the surface [12]. This dense surface caused by the presence of additional material that fills the pores [9]. It can also be seen that the rough shape material was a metal that sticks to the surface. Then, this result further identified using EDX as can be seen from spectrum in Figure 4. EDX spectrum shows the Fe, Cr, S, Ni, O, and C elements over the stainless steel substrate. Fe and Cr elements that appear on the spectrum come from stainless steel, while C and S come from PANI. Ni and O have high percentage which indicated that this materials contain NiO attached over the PANI surface. This SEM-EDX results confirmed that PANI-NiO was successfully synthesized.

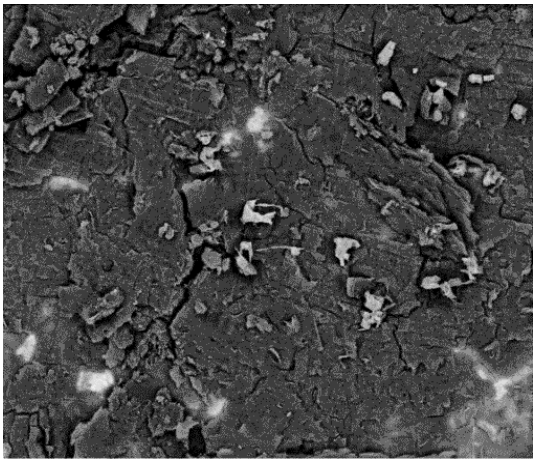

Figure 3. Micrograph of PANI-NiO

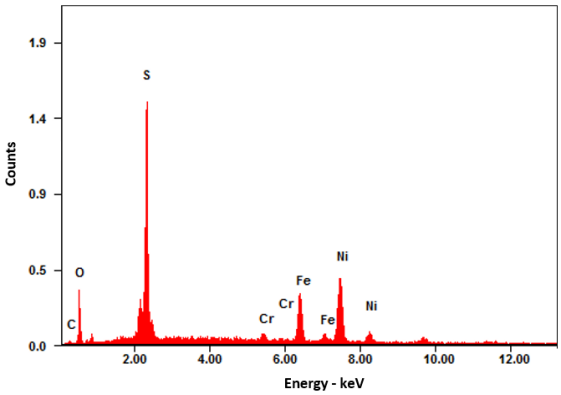

Figure 4. EDX spectrum of PANI-NiO

3.4 Capacitance Test

Based on Table 1, it can be seen that NiO increases the capacitance value of the material. This is because NiO improves the conductivity at the electrode which results in a higher adsorption effect on the PANI-NiO [21]. Based on this, combination of PANI and NiO materials will increase the capacitance properties of the material.

Sample	Specific Capacitance (F/g)
PANI	75
PANI-NiO	98

Table 1. Capacitance of PANI and PANI-NiO

Figure 5 shows the PANI-NiO capacitance values with potentials of 1.00 V, 1.25 V, 1.50 V, 1.75 V, and 2.20 V. Potentials of 1.00 V and 1.25 V produce 295.67 F/g and 475.24 F/g values of capacitance, respectively, that larger among the other three samples. Both have larger

capacitance due to the low potential during synthesis, results in a thinner and more even surface of the film, thus improve electroactive properties of the material as a charge storage [22]. The electroactive properties of the material can increase the conductivity which affects the activity of ions or molecules in the electrolyte solution [23].

PANI-NiO at potentials of 1.50 V, 1.75 V, and 2.20 V results in lower capacitances, namely 161.9 F/g, 70.1 F/g, and 4.6 F/g, respectively. This is because the high potential during synthesis will reduce the efficient interaction between the electrodes and ions [8]. Based on literatures, the large capacitance can increase the absorption process in the material [8]. The greater the capacitance value, the higher the absorption process in a material. The ion absorption process in the material affects the application performance on the material and this data is closely related to the resistance value in the material which will be discussed in the impedance discussion [21].

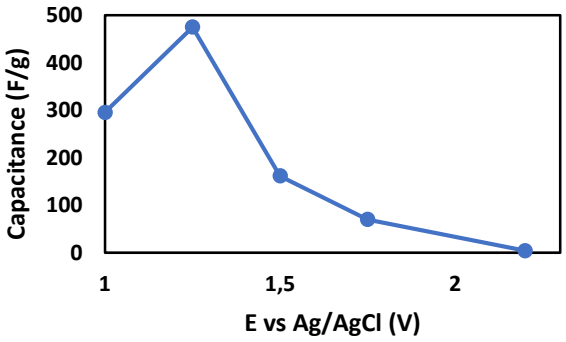

Figure 5. Specific capacitance of PANI-NiO at different potentials

3.5 Impedance Test

Figure 6 shows the Nyquist plot of PANI-NiO synthesized with different potentials. In general, the higher the potential during synthesis, the larger the R_{ct}. This is evidenced by the calculation of R_s and R_{ct} generated on the material shown in Figure 7.

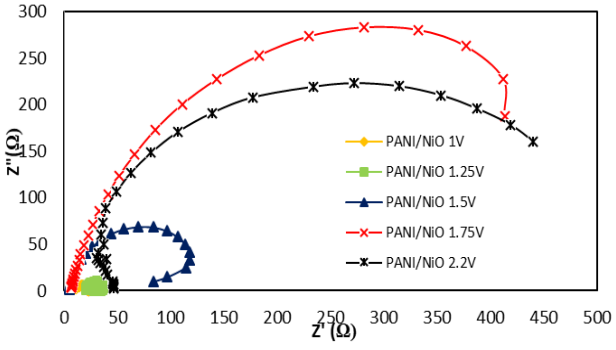

Figure 6. Nyquist plot of PANI-NiO with different potentials

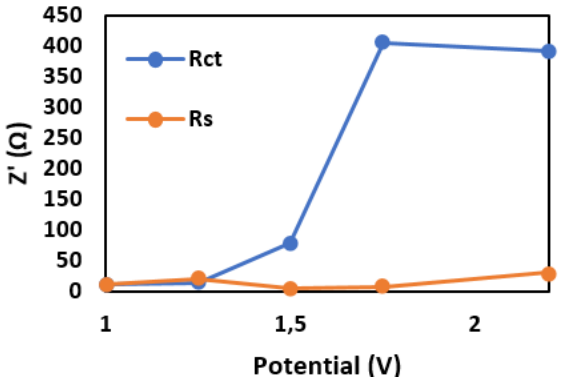

Figure 7. R_s dan R_{ct} of PANI-NiO

Based on the impedance data, PANI/NiO prepared at 1.00 V has the smallest resistance value for the double layer which affects the occurrence of a good charge intercalation and deintercalation process [14]. This can support data from capacitance, namely for PANI-NiO 1.00 V and 1.25 V that have high adsorption capacity, followed by PANI-NiO prepared at 1.50 V, 1.75 V, and 2.20 V.

3.6 Capacity Deionization Test

Figure 8 shows the conductivity of PANI-NiO synthesized at different potentials for 1800 s. The conductivity at the PANI-NiO 1.00 V decrease until 1635 s with a value of 11.12 mS, then increased to 11.14 mS. The conductivity of PANI-NiO 1.25 V constantly decreased for 1800 s. At the PANI-NiO 1.50 V, it can be seen that the conductivity continues to decrease for 1185 s, then increases after 1200 s with a conductivity value of 11.61 mS to 11.62 mS. At the PANI-NiO 1.75 V and 2.20 V, the conductivity constantly decreased for 1800 s. In general, PANI-NiO electrode show that as the adsorption time increases, the electroadsorption will decrease. This is because the electrode surface has been filled with ions, so the efficiency of ion reduction decrease. The value of salt reduction efficiency is calculated by Eq. 1.

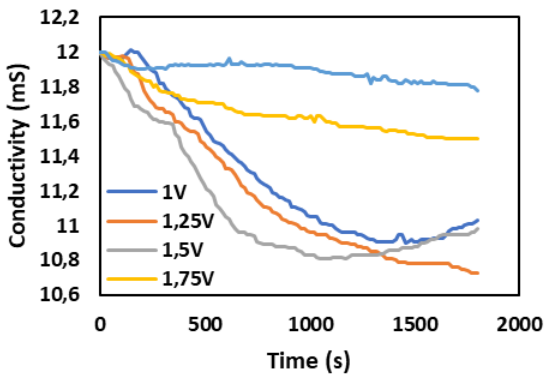

Figure 8. Desalination test of PANI-NiO

Figure 9 displays the efficiency of reducing salt at the PANI-NiO electrode from materials synthesized at different potentials. It can be seen that the highest salt reduction efficiency occurs at 1.25 V with a percentage value of 9.95%, while for the potentials of 1.00 V, 1.50 V, 1.75 V, and 2.20 V, the percentage of salt reduction was 8.03%, 8.13%, 3.87%, and 1.79%, respectively.

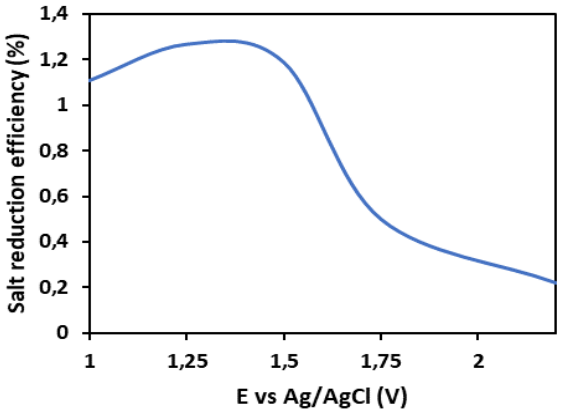

Figure 9. Salt reduction efficiency of PANI-NiO

4. Conclusion

PANI-NiO was successfully synthesized by electrodeposition method with different applied potentials, which has been confirmed by FTIR and XRD data. Based on the SEM-EDX data, PANI-NiO has a tightly stacked granular morphology, which consist of Fe, Cr, S, Ni, O, and C elements. The large value of capacitance will result in a greater charge transfer, which improve the adsorption performance of the material. A good impedance will produce small resistance, which will increase the electrolytic charge adsorption process so that the adsorption performance increases. Owing to its high capacitance, low charge transfer resistance, and high salt reduction capacity, the PANI-NiO prepared at 1.25 V might be a potential material to be developed for the electrolyte deionization application.

Acknowledgement

This work was funded by Kementerian Riset, Teknologi, dan BRIN Republik Indonesia through research grant No. 27/SP2H/DRPM/LPPM-UNJ/III/2019.

References

[1] Kaminski, W., Marszalek, J., & Tomczak, E. (2018). Water desalination by pervaporation – Comparison of energy consumption. Desalination, 433, 89–93.

[2] Porada, S., Zhao, R., van der Wal, A., Presser, V., & Biesheuvel, P. M. (2013). Review on the science and technology of water desalination by capacitive deionization. Prog. Mater. Sci., 58(8), 1388–1442.

[3] Oren, Y. (2008). Capacitive deionization (CDI) for desalination and water treatment — past , present and future (a review). 228, 10–29.

[4] Yoon, H., Lee, J., Kim, S. R., Kang, J., Kim, S., Kim, C., & Yoon, J. (2016). Capacitive deionization with Ca-alginate coated-carbon electrode for hardness control. Desalination, 392, 46–53.

[5] Zhao, R., Porada, S., Biesheuvel, P. M., & Van der Wal, A. (2013). Energy consumption in membrane capacitive deionization for different water recoveries and flow rates, and comparison with reverse osmosis. Desalination, 330, 35–41.

[6] Park, K. K., Lee, J. B., Park, P. Y., Yoon, S. W., Moon, J. S., Eum, H. M., & Lee, C. W. (2007). Development of a carbon sheet electrode for electrosorption desalination. Desalination, 206(1–3), 86–91.

[7] Male, U., Singu, B. S., & Srinivasan, P. (2015). Aqueous, interfacial, and electrochemical polymerization pathways of aniline with thiophene: Nano size materials for supercapacitor. Journal of Applied Polymer Science, 132(22), 1–8.

[8] Navale, Y. H., Navale, S. T., Dhole, I. A., Stadler, F. J., & Patil, V. B. (2018). Specific capacitance, energy and power density coherence in electrochemically synthesized polyaniline-nickel oxide hybrid electrode. Organic Electronics, 57, 110–117.

[9] Azharudeen, A. M., Karthiga, R., Rajarajan, M., & Suganthi, A. (2019). Fabrication, characterization of polyaniline intercalated NiO nanocomposites and application in the development of non-enzymatic glucose biosensor. Arabian Journal of Chemistry, 625, 124-136.

[10] Prasankumar, T., Wiston, B. R., Gautam, C. R., Ilangovan, R., & Jose, S. P. (2018). Synthesis and enhanced electrochemical performance of PANI/Fe3O4nanocomposite as supercapacitor electrode. Journal of Alloys and Compounds, 757, 466–475.

[11] Gonzalez, M. B., & Saidman, S. B. (2011). Electrodeposition of polypyrrole on 316L stainless steel for corrosion prevention. Corrosion Science, 53(1), 276–282.

[12] Velhal, N., Patil, N., Jamdade, S., & Puri, V. (2014).

Studies on galvanostatically electropolymerised polypyrrole/polyaniline composite thin films on stainless steel. Applied Surface Science, 307, 129–135.

[13] Bandgar, D. K., Khuspe, G. D., Pawar, R. C., Lee, C. S., & Patil, V. B. (2012). Facile and novel route for preparation of nanostructured polyaniline (PANi) thin films. Applied Nanoscience, 4(1), 27–36.

[14] Mi, H., Zhang, X., Ye, X., & Yang, S. (2008). Preparation and enhanced capacitance of core-shell polypyrrole/polyaniline composite electrode for supercapacitors. Journal of Power Sources, 176(1), 403–409.

[15] Han, J. J., Cheng, J. N., Pan, F. W., Liu, X. K., & Zhang, F. (2013). Effect of Synthesis Process of Polyaniline for the Zn-PANi Secondary Batteries. Advanced Materials Research, 608–609, 1342–1346.

[16] Sonavane, A. C., Inamdar, A. I., Deshmukh, H. P., & Patil, P. S. (2010). Multicoloured electrochromic thin films of NiO/PANI. Journal of Physics D: Applied Physics, 43(31).

[17] Maity, P. C., & Khandelwal, M. (2016). Synthesis Time and Temperature Effect on Polyaniline Morphology and Conductivity. American Journal of Material Synthesis and Processing, 1(4), 37–42.

[18] Lei, W., He, P., Zhang, S., Dong, F., & Ma, Y. (2014). One-step triple-phase interfacial synthesis of polyaniline-coated polypyrrole composite and its application as electrode materials for supercapacitors. Journal of Power Sources, 266, 347–352.

[19] Xu, H., Li, X., & Wang, G. (2015). Polyaniline nanofibers with a high specific surface area and an improved pore structure for supercapacitors. Journal of Power Sources, 294, 16–21.

[20] Budi, S., Fitri, E., Paristiowati, M., Cahyana, U., Pusparini, E., Nasbey, H., & Imaddudin, A. (2016). Surface area and conductivity of polyaniline synthesized under UV irradiation. Journal of Physics: Conference Series, 172(012049), 1–7.

[21] Zhao, J., Tian, Y., Liu, A., Song, L., & Zhao, Z. (2019). The NiO electrode materials in electrochemical capacitor: A review. Materials Science in Semiconductor Processing, 96(189), 78–90.

[22] Eftekhari, A., Li, L., & Yang, Y. (2017). Polyaniline supercapacitors. Journal of Power Sources, 347, 86–107.

[23] Balint, R., Cassidy, N. J., & Cartmell, S. H. (2014). Conductive polymers: Towards a smart biomaterial for tissue engineering. Acta Biomaterialia, 10(6), 2341–2353.

[24] Chen, Y., & Manzhos, S. (2016). Potential and capacity control of polyaniline based organic cathodes: An ab initio study. Journal of Power Sources, 336, 126–131.